

Shell Model Calculations on Natural Parity States in $10 \leq A \leq 14$ Nuclei

R. Saayman, P. R. de Kock and J. H. van der Merwe

Merensky Institute for Physics, University of Stellenbosch,
Stellenbosch, Republic of South Africa

Received June 27, 1973

Shell model calculations of natural parity states in the $10 \leq A \leq 14$ mass region have been performed by assuming an inert ${}^4\text{He}$ core with the residual interaction in the $1p$ shell only. The modified surface delta interaction (MSDI) has been used as an effective two-body interaction. The MSDI parameters as well as the single-particle binding energies have been deduced from a least-squares fit to experimentally known levels in, firstly, the separate ${}^{10}\text{B}$, ${}^{11}\text{B}-\text{C}$, ${}^{12}\text{C}$, ${}^{13}\text{C}-\text{N}$ and ${}^{14}\text{N}$ nuclei, and secondly, the whole mass region $10 \leq A \leq 14$. Multipole moments for ground states and $M1$ and $E2$ radiative widths for excited states have been calculated with the resultant wave functions.

1. Introduction

In terms of the shell model, nuclei in the mass region $5 \leq A \leq 15$ can be assumed to consist of a closed ${}^4\text{He}$ core plus $(A-4)$ extra-core nucleons moving in the $1p$ -shell orbital. Such $(1s)^4(1p)^{A-4}$ configurations will give rise to states of natural parity, $\pi = (-1)^A$, only. A detailed shell-model calculation on this basis has been performed by Cohen and Kurath [1], who empirically obtained two-body matrix elements in both the LS - and jj -coupling approximations from fitting level energies. An effective interaction obtained from the Hamada-Johnstone potential was used by Halbert, Kim and Kuo [2] to calculate spectra for $1p$ -shell nuclei.

Since these two theoretical structure studies, considerable new experimental data on these nuclei have been accumulated (see the compilations of Ajzenberg-Selove and Lauritsen [3–5] and additional references at Fig. 3) which justify a recalculation of the low-lying level structures. Following the success of the modified surface delta interaction (MSDI) in calculations [6–14] on $2s-1d$ shell nuclei, it is also worthwhile to investigate the behaviour of this zero-range two-body surface force towards the lighter mass region.

Only nuclei in the mass region $10 \leq A \leq 14$ are included in the present study. The lower limit follows from the assumption that the jj -coupling scheme is a good approximation in the upper half of the $1p$ shell. The upper mass limit is necessary, since no admixtures from the higher-lying

$2s-1d$ shell are allowed in the present model space. Only natural parity states which can be accounted for by predominantly $1p$ -shell configurations, are considered here. Due to the obvious inadequacy of such a restricted model to account for the structure of mass-15 nuclei, these nuclei will be dealt with in a subsequent paper, which will discuss a systematic model space expansion to the $2s-1d$ shell.

2. Computational Procedure

Assuming a distribution of n nucleons in the $1p_{3/2}$ subshell and m nucleons in the $1p_{1/2}$ subshell with $n+m=A-4$, the many-body residual interaction of this model space is expressed as a linear combination of two-body matrix elements by using standard decomposition methods as described in Refs. [15–17]. Using the jj -coupling scheme, the interaction energy will then depend on fifteen such two-body matrix elements (ten diagonal and five off-diagonal elements), as well as the two single-particle energies $E(1p_{3/2})$ and $E(1p_{1/2})$. In their calculations Cohen and Kurath [1] treated all these quantities as free parameters. In the present investigation the necessary two-body matrix elements are expressed in terms of the modified surface delta interaction defined [18, 19] by

$$V_{ij}(\text{MSDI}) = -4\pi A_T \delta(\Omega_{ij}) \delta(r_i - R) \delta(r_j - R) + B_T, \quad (1)$$

where Ω_{ij} is the angular coordinate between the interacting particles i and j , and R the nuclear radius. Employing this interaction drastically reduces the number of effective parameters to a maximum of six: the four interaction strength parameters, A_0 , A_1 , B_0 and B_1 , the subscripts indicating the isospin of the coupled nucleon pair, as well as the two single-particle energies. The theoretical level energies are obtained as usual from a diagonalization of the constructed interaction matrices for different J, T values. An optimisation of the parameters of the interaction elements is executed to yield the best fit of the eigenvalues to the experimental level energies corrected for Coulomb and core energies. The present structure study was performed in two stages. In the preliminary calculations (denoted as calculations I), each mass number in the region $10 \leq A \leq 14$ was treated separately in order to make a selection of levels within the chosen shell model space, as well as to study the variation of the parameters with mass number. The energy states relative to its ground state were calculated and fitted for each individual nucleus. Only four free parameters appeared in the calculations: the SDI strengths A_0 and A_1 , the single-particle energy splitting $\Delta E(1p_{1/2} - 1p_{3/2})$ and the difference $(B_1 - B_0)$ which is necessary to account for the splitting between groups of levels with different isospin $T = T_Z$ and $T = T_Z + 1$.

In the final calculation (denoted as calculation II) a combined investigation was carried out in excited as well as ground states over the

whole mass region $10 \leq A \leq 14$. In this case it was necessary to correct all experimental level energies E to be fitted for both the internal energy E_c of the ${}^4\text{He}$ core and the Coulomb energy E_C of all particles outside the core. Assuming charge independence of nuclear forces, values of E_C were obtained from the difference in binding energies of mirror nuclei in the region $5 \leq A \leq 15$ by applying the semi-empirical formulae given by de-Shalit and Talmi (Eqs. (30.2) and (30.3) of Ref. [16]). To a first order approximation it was assumed that the Coulomb corrections would be similar for the ground state and all the corresponding excited states in the same nucleus. In calculation II all six parameters $A_0, A_1, B_0, B_1, E(1p_{3/2})$ and $E(1p_{1/2})$ were fitted simultaneously.

3. Effective Interaction Parameters

From the final parameter values obtained in the energy fits of calculations I and II, Fig. 1 is drawn to illustrate the mass number depend-

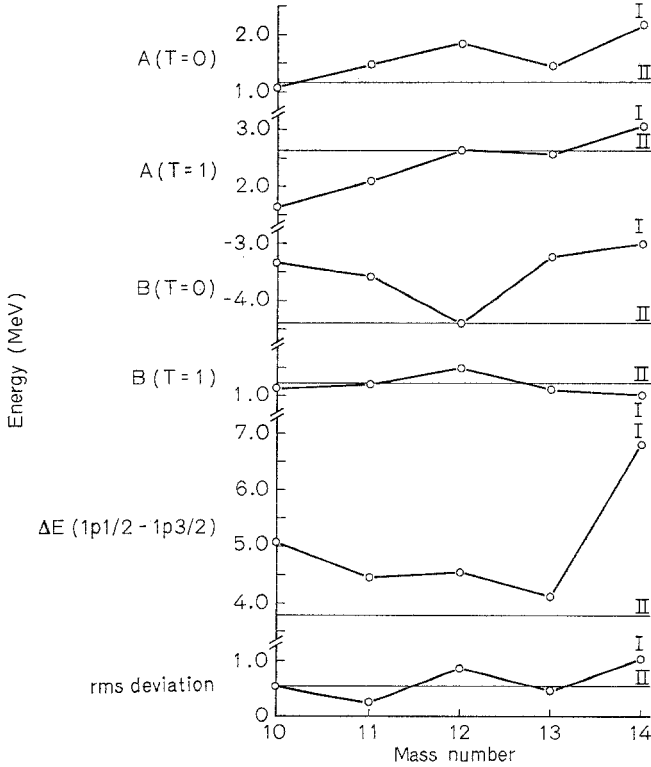


Fig. 1. Variation of the interaction parameters and the root mean square deviation with increase in mass number

ence of the MSDI strengths and the single-particle energy splitting. As measure of the quality of the separate energy fits, the root mean square deviation [16] between calculated and experimental level energies is also displayed (bottom graph). Its value of 0.55 MeV in calculation II points to good agreement between the present theory and experiment. Regarding the individual cases of calculation I, the best agreement was obtained for the uneven A nuclei. The poorer results in the case of $A=12$ are to be expected since the levels of ^{12}C included in this fit, covered a much wider energy range (~ 20 MeV) than in the other nuclei. The poor agreement in the $A=14$ case should be explained in terms of the very restricted $1p$ -shell model space available for this mass number, as well as the proximity of the $2s-1d$ shell.

From the results of calculations I in Fig. 1 follow that the binding energy difference between the $1p_{3/2}$ and $1p_{1/2}$ orbitals appears to be reasonably constant over the $10 \leq A \leq 13$ mass region. Except for ^{14}N , the calculated splittings compare favourably with values (in MeV) 3.90 for ^{10}B , 3.14 for ^{11}B , 4.21 for ^{12}C , 3.61 for ^{13}N and 3.14 for ^{14}N , calculated [2] from the effective t -matrix interaction between the $1s$ and $1p$ nucleons. The absolute single particle energies resulting from calculation II are $E(1p_{3/2})=0.45$ MeV and $E(1p_{1/2})=4.23$ MeV, and are somewhat lower than the values of 0.96 and 5.60 MeV obtainable from the empirical energy spectrum of ^5He . However, these latter values presume the ground and first excited states in this core-plus-neutron nucleus as pure single-particle levels.

From the results of calculations I the SDI strengths A_0 and A_1 are shown to increase gradually with mass number. A gradual mass dependence of these parameters has also been found in the $2s-1d$ shell. Calculation II rendered the values $A_0=1.15$ MeV and $A_1=2.64$ MeV. In calculations I the relative modification parameter (B_1-B_0) was necessary to account properly for the splitting between $T=T_Z$ and $T=T_Z+1$ levels. Except for a major discrepancy in the $A=12$ case, this parameter value showed little variation over the mass region $10 \leq A \leq 14$ (not illustrated in Fig. 1), the average value being ~ 4.7 MeV. In the combined calculation II, where apart from the above spacings, the binding energies of nuclei with different mass numbers were also fitted, the two parameters B_0 and B_1 were independently varied. The final values obtained are $B_0=-4.38$ MeV and $B_1=1.21$ MeV, which yield a difference reasonably close to that obtained in calculations I. This consistence as well as the relation between these two B_T values suggest that the B_T term in Eq. (1), which was added to the SDI on purely empirical grounds, can be replaced by a term $B(\tau_i \cdot \tau_j)$. Such a term has naturally a much better physical justification and introduces only one strength parameter B instead of the former two, B_0 and B_1 . The above-mentioned values of B_1-B_0 then lead

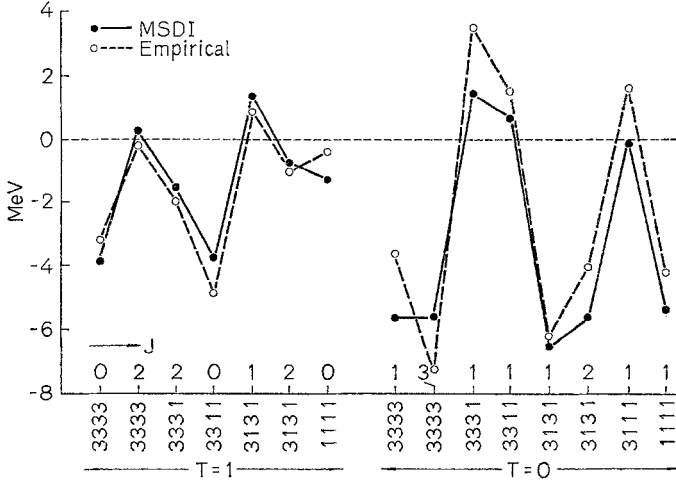


Fig. 2. Values of the two-body matrix elements calculated from the MSDI are compared with those obtained empirically [1]. The nj values are specified by 3 for $1p_{3/2}$ and 1 for $1p_{1/2}$. The notation 3331, for example, denotes the matrix element $\langle 33 | V | 31 \rangle$.

to a fairly constant B value (~ 1.25 MeV) over the whole mass region and yield separate B_0 and B_1 values for each mass number. These are compared in Fig. 1 with the values separately fitted in calculation II.

With the MSDI parameters obtained in calculation II, the fifteen two-body matrix elements of the $1p$ shell, which were used as free parameters by Cohen and Kurath [1], can be computed. The good agreement between these two sets of matrix elements as displayed in Fig. 2, indicates that the modified surface delta interaction is a good approximation of the effective two-body interaction in light nuclei.

4. Energy Spectra and Wave Functions

The theoretical level schemes as obtained in calculations I and II are compared in Fig. 3 with the experimental spectrum for each mass number in the $10 \leq A \leq 14$ region. From the results of calculation II, Table 1 compares the computed and experimental ground state energies relative to the ^4He core, after the Coulomb energy of all outside particles has been subtracted. The experimental and calculated excitation energies of the states selected for the energy fits are presented in Table 2. For these states the dominant shell model configuration in its structure is also cited.

In the following sections, some restrictions and results of the calculations will be discussed more in detail:

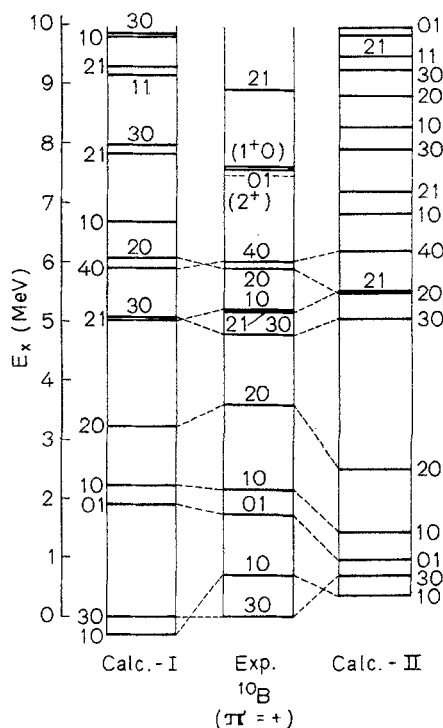


Fig. 3. The calculated and experimental level schemes for nuclei in the $10 \leq A \leq 14$ mass region, showing only natural parity states. Levels of even-mass nuclei are identified by J, T values; levels of odd-mass nuclei are identified by J values and have $T = 1/2$, unless stated otherwise. The experimental data are from the compilations of Ajzenberg-Selove and Lauritsen [3–5], with some additions and modifications from Refs. [20–23] for $A = 10$, Refs. [24–28] for $A = 11$, Refs. [29–33] for $A = 12$, Refs. [34–36] for $A = 13$ and Refs. [37–41] for $A = 14$. The positions of the fitted levels and the corresponding experimental levels are inter-connected by dashed lines. Low-lying levels which were omitted in the energy fits, are discussed in the text. For the odd-mass mirror pairs $^{11}\text{B} - \text{C}$ and $^{13}\text{C} - \text{N}$ the average energies were used in the least-squares fitting procedure, without allowing for secondary energy differences between corresponding levels, e.g. Coulomb energy differences and Thomas-Ehrman shifts. Hatched areas indicate high level density

4.1. Spectrum of $A = 10$

The energy fit to nine positive-parity levels in ^{10}B is fairly good, the worst disagreement being a failure of the present theory to reproduce the observed ordering of the $JT = 30$ ground and $JT = 10$ first excited states. The observed 5.18 MeV positive-parity level with $JT = 10$ was not included in the energy fit, because of experimental evidence [42] that its predominant configuration is not p^6 . In the present study the third

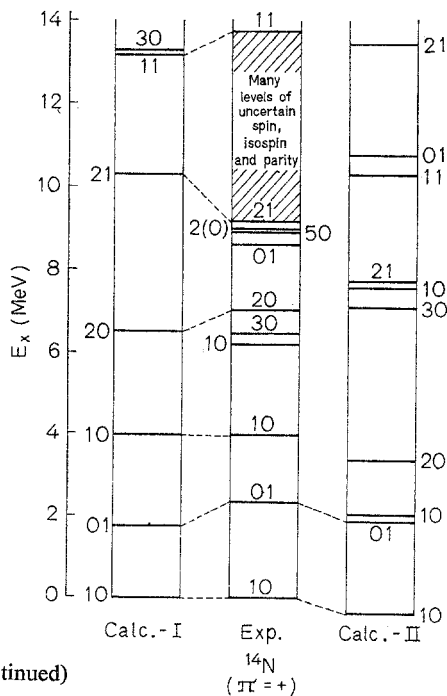
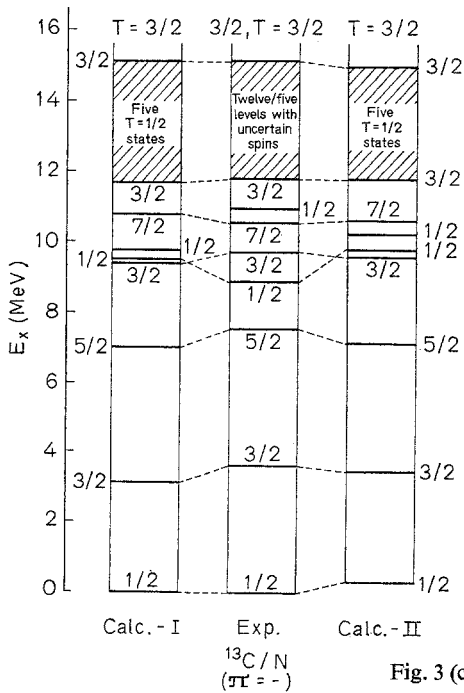
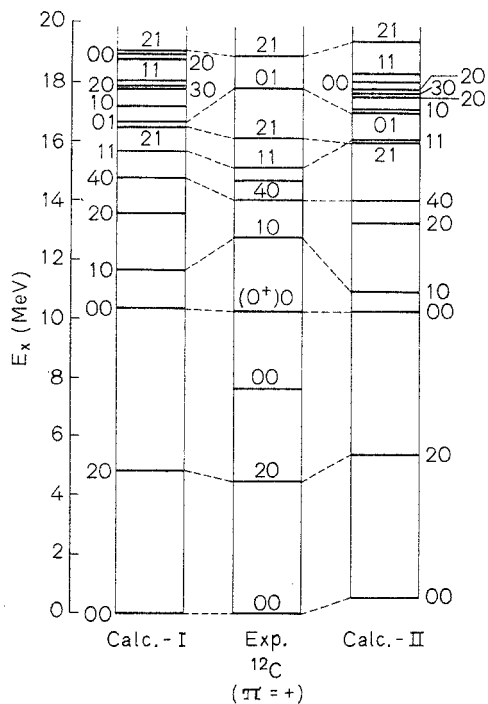
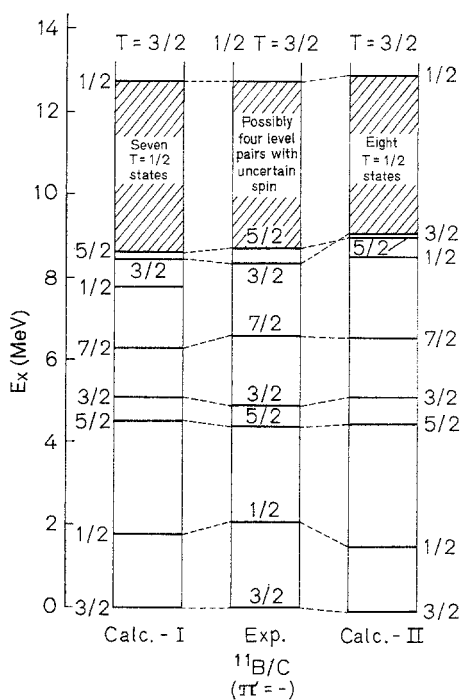


Fig. 3 (continued)

Table 1. Comparison of calculated and empirical ground state energies relative to the ${}^4\text{He}$ core and with the Coulomb energy of all particles outside the core subtracted

<i>A</i>	Nucleus	Ground state J^π, T	$E - E_c - E_C$	
			Theory	Experiment
10	Be	$0^+, 1$	-39.91	-39.17
	B	$3^+, 0$	-40.17	-40.89
	C	$0^+, 1$	-39.91	-39.13
11	Be	$1/2^-, 3/2$	-39.43	-39.67
	B	$3/2^-, 1/2$	-52.38	-52.35
	C	$3/2^-, 1/2$	-52.38	-52.22
12	B	$1^+, 1$	-54.90	-55.72
	C	$0^+, 0$	-70.43	-70.94
	N	$1^+, 1$	-54.90	-55.78
13	B	$3/2^-, 3/2$	-60.91	-60.60
	C	$1/2^-, 1/2$	-75.57	-75.88
	N	$1/2^-, 1/2$	-75.57	-75.87
14	C	$0^+, 1$	-84.56	-84.06
	N	$1^+, 0$	-86.71	-86.42
	O	$0^+, 1$	-84.56	-84.08

Table 2. Low-lying natural parity states in $10 \leq A \leq 14$ nuclei arising from pure $1p$ -shell configurations*

State		Excitation energy (in MeV)			Dominant shell-model structure		
T	J^π	Experimental	Calculated		Configuration	Strength (%)	
			I	II		I	II
$A=10$; Nucleus: B							
0	1^+	0.72	-0.32	0.37	$p_{10}^6 p_{00}^0$	81	69
		2.15	2.21	1.45	$p_{3/2, 1/2}^5 p_{1/2, 1/2}^1$	80	77
	2^+	3.59	3.21	2.52	$p_{3/2, 1/2}^5 p_{1/2, 1/2}^1$	88	83
		5.92	6.08	5.49	$p_{5/2, 1/2}^5 p_{1/2, 1/2}^1$	52	29
					$p_{21}^4 p_{01}^2$	33	46
	3^+	0.00	0.00	0.00	$p_{30}^6 p_{00}^0$	84	71
4.77		5.07	5.07	$p_{5/2, 1/2}^5 p_{1/2, 1/2}^1$	72	55	
1	4^+	6.03	5.81	6.20	$p_{7/2, 1/2}^5 p_{1/2, 1/2}^1$	94	85
	0^+	1.74	1.90	0.98	$p_{01}^6 p_{00}^0$	82	61
	2^+	5.17	5.01	5.53	$p_{21}^6 p_{00}^0$	76	41

* The levels cited are those used in the least squares fitting procedure of the individual mass numbers (calculation I). Experimental levels followed by † were omitted in the combined fit of the $10 \leq A \leq 14$ mass region (calculation II). In the configuration notation the first and second *p* designates the $1p_{3/2}$ and $1p_{1/2}$ subshells respectively. The probability strengths given are defined as the squares of the shell-model amplitudes $\times 100\%$.

Table 2 (continued)

State		Excitation energy (in MeV)					Dominant shell-model structure		
T	J^π	Experimental			Calculated		Configuration	Strength (%)	
					I	II		I	II
$A=11$;									
<i>Nuclei:</i>									
		B	C	B/C					
1/2	1/2 ⁻	2.12	2.00	2.06	1.72	1.48	$p_{01}^6 p_{1/2,1/2}^1$	62	59
	3/2 ⁻	0.00	0.00	0.00	0.00	0.00	$p_{3/2,1/2}^7 p_{00}^0$	65	57
		5.02	4.79	4.91	5.14	5.10	mixture		
		8.57	8.11	8.34	8.46	9.05	mixture		
	5/2 ⁻	4.44	4.31	4.38	4.51	4.45	$p_{21}^6 p_{1/2,1/2}^1$	67	59
		8.93	8.42	8.68	8.63	8.99	$p_{30}^6 p_{1/2,1/2}^1$	74	4
							$p_{3/2,1/2}^5 p_{10}^2$	6	73
	7/2 ⁻	6.74	6.48	6.61	6.34	6.54	$p_{30}^9 p_{1/2,1/2}^1$	79	73
3/2	1/2 ⁻	13.02	12.45	12.74	12.74	12.85	$p_{01}^8 p_{1/2,1/2}^1$	88	86
$A=12$; <i>Nucleus:</i> C									
0	0 ⁺		0.00		0.00	0.00	$p_{00}^8 p_{00}^0$	36	44
							$p_{01}^6 p_{01}^2$	42	41
			10.30		10.32	10.30	$p_{00}^8 p_{00}^0$	54	46
	1 ⁺		12.71		11.60	10.94	$p_{3/2,1/2}^7 p_{1/2,1/2}^1$	68	67
	2 ⁺		4.44		4.81	5.34	$p_{3/2,1/2}^7 p_{1/2,1/2}^1$	47	51
	4 ⁺		14.08		14.80	14.00	$p_{30}^9 p_{10}^2$	76	76
1	0 ⁺		17.77		16.64	16.97	$p_{01}^8 p_{01}^2$	93	95
	1 ⁺		15.11		15.70	16.04	$p_{3/2,1/2}^7 p_{1/2,1/2}^1$	69	75
	2 ⁺		16.11		16.47	15.96	$p_{3/2,1/2}^7 p_{1/2,1/2}^1$	83	82
			18.84		18.98	19.34	$p_{21}^6 p_{01}^2$	64	67
$A=13$;									
<i>Nuclei:</i>									
		B	C	B/C					
1/2	1/2 ⁻	0.00	0.00	0.00	0.00	0.00	$p_{00}^8 p_{1/2,1/2}^1$	70	69
		8.86	8.92	8.89	9.51	9.79	$p_{01}^6 p_{1/2,1/2}^3$	43	43
	3/2 ⁻	3.68	3.51	3.60	3.12	3.44	$p_{3/2,1/2}^7 p_{01}^2$	61	61
		9.90	9.52	9.71	9.45	9.59	$p_{3/2,1/2}^7 p_{10}^2$	75	76
		11.72	11.87	11.80	11.68	11.74	$p_{10}^9 p_{1/2,1/2}^3$	23	39
							$p_{21}^6 p_{1/2,1/2}^3$	45	32
	5/2 ⁻	7.55	7.39	7.47	7.04	7.14	$p_{3/2,1/2}^7 p_{10}^2$	89	87
	7/2 ⁻	10.75	10.36	10.56	10.81	10.60	$p_{30}^9 p_{1/2,1/2}^3$	90	88
3/2	3/2 ⁻	15.11	15.07	15.09	15.09	14.97	$p_{3/2,1/2}^7 p_{01}^2$	92	91
$A=14$; <i>Nucleus:</i> N									
0	1 ⁺		0.00		0.00	0.00	$p_{00}^8 p_{10}^2$	98	98
			3.95 [†]		3.97	2.03	$p_{3/2,1/2}^7 p_{1/2,1/2}^3$	92	92
	2 ⁺		7.03 [†]		6.51	3.34	$p_{3/2,1/2}^7 p_{1/2,1/2}^3$	100	100
1	0 ⁺		2.31		1.73	1.86	$p_{00}^8 p_{01}^2$	89	77
	1 ⁺		13.75 [†]		13.15	10.30	$p_{3/2,1/2}^7 p_{1/2,1/2}^3$	100	100
	2 ⁺		9.17 [†]		10.33	7.76	$p_{3/2,1/2}^7 p_{1/2,1/2}^3$	96	93

$JT=10$ state is predicted near 7 MeV excitation. This state might probably be associated with the observed level at 7.62 MeV, which features an uncertain $(1^+, 0)$ assignment in Ref. [3].

The observed $T=0$ level at 4.77 MeV has been given the probable (2^+) assignment in Ref. [3]. Similar as was found in previous theoretical studies [1, 2], this level is difficult to fit as a $JT=20$ state. Cohen and Kurath [1] suggested a 3^+ spin-parity assignment which is definitely confirmed by the present calculations, as well as by newer experimental data [20–22]. The $T=1$ isobaric analogues of the 0^+ ground and 2^+ first excited states of ^{10}Be and ^{10}C are both well-accounted for in terms of the present theory.

4.2. Spectrum of $A=11$

As displayed in Fig. 3, excellent agreement between theory and experiment is obtained in the case of the eight low-lying negative-parity states of the $^{11}\text{B} - ^{11}\text{C}$ mirror pair. From Table 1 follows that the calculated and empirical energies for the ground states differ only slightly. The $T=3/2$ analogue of the $1/2^-$ ground state in ^{11}Be is also well reproduced at 12.74 MeV excitation, which nearly averages its observed energy [4, 24, 28] in ^{11}B (13.02 MeV) and ^{11}C (12.45 MeV).

Regarding the $T=1/2$ excited states, the present investigation favours a definite $J^\pi=3/2^-$ assignment to the observed mirror levels at 8.57 MeV in ^{11}B and 8.11 MeV in ^{11}C . This clears the uncertainty $J^\pi \leq 5/2^-$ given by Ajzenberg-Selove and Lauritsen [4] and confirms the experimental results of Fortune *et al.* [25] who obtained a unique $3/2^-$ assignment for the level in ^{11}C from a study of single-particle transfer reactions $^{10}\text{B}(^3\text{He}, d)^{11}\text{C}$ and $^{12}\text{C}(^3\text{He}, \alpha)^{11}\text{C}$.

4.3. Spectrum of $A=12$

Of particular interest in the positive-parity spectrum of ^{12}C are the states with zero spin and isospin. Apart from the well-known ground state, two excited states can be identified as belonging to this group. The second excited state at 7.66 MeV was omitted from the present energy fits on account of published evidence [43, 1, 29] that its predominant configuration contains an admixture from the $2s-1d$ shell. From the results of both calculations I and II (Fig. 3 and Table 2), the observed level at 10.30 MeV is exactly predicted as the second $JT=00$ state with pure p -shell configurations. It is found to have a dominant $p_{00}^8 p_{00}^0$ structure component in its wave function.

With regard to the shell-model structure of the other fitted levels, previous theoretical results, as summarized by Ball and Cerny [29], are confirmed, with more definite predictions in the case of the 14.08 MeV $(4^+, 0)$, 17.77 MeV $(0^+, 1)$ and 18.84 MeV $(2^+, 1)$ levels, which have previously only been vaguely classified as p^8 -shell model states.

4.4. Spectrum of $A=13$

In the energy fit to the negative-parity spectrum of the $^{13}\text{C}-^{13}\text{N}$ mirror pair, two unpaired levels (not shown in Fig. 3) had to be omitted: the level at 9.50 MeV in ^{13}C with uncertain $(3/2^-)$ assignment, and the $5/2^-$ level at 10.35 MeV in ^{13}N . Except for the inverted order of the second $1/2^-$ and $3/2^-$ states, good agreement between theory and experiment is obtained in the present case. A third $1/2^-$ state is predicted directly above the second, but could not successfully be identified as the observed pair at 11.08 and 10.78 MeV in ^{13}C and ^{13}N respectively. This probably indicates that a $2s-1d$ component should be admixed to the dominant $[29] p^9$ configuration of this pair. The presence of several low-lying non-normal parity states in the $A=13$ nuclei (see description in Ref. [35]) also indicates the importance of the $2s-1d$ shell already at this low mass number.

All other excited states with spin $> 1/2$ are well reproduced. This also applies to the $T=3/2$ isobaric analogue of the ^{13}B ground state. The dominant configurations (Table 2) differ from previous theoretical results in the case of the second $1/2^-$ and third $3/2^-$ states, which both feature a dominant $p_{3/2,1/2}^7 p_{10}^2$ component in the compilation of Ref. [29].

4.5. Spectrum of $A=14$

In view of the limited configuration space and the proximity of the $2s-1d$ shell, it is to be expected that the present model can only give a restricted description of the positive-parity level scheme of ^{14}N . In the data selection the two closelylying $T=0$ levels at 6.20 MeV (1^+) and 6.44 MeV (3^+) were not considered for the energy fits in view of published evidence [29, 44] that $2s-1d$ components are strongly present.

Although calculation I generally reproduces the level order of the six most probable states featuring pure p -shell configurations correctly (Fig. 3), more attention should be paid to the results of calculation II where more experimental data were employed in the least squares fit. In order to minimize the probability of $2s-1d$ admixing, only the lowest $T=0$ and 1 levels of ^{14}N (respectively the ground and 2.31 MeV first excited states) were included in this case. Although the correct level order of ^{14}N is preserved in calculation II, the observed energy spacings are not reproduced between levels predicted above the two fitted levels. It is also interesting to note that the asserted $2s-1d$ -shell components of the first $JT=30$ and third 10 states mentioned above, do not have a marked effect on their energy values. The dominant configurations of previous theoretical studies [29] are confirmed by the present calculations (Table 2), with additional information being offered in the case of the 9.17 MeV level with $JT=21$.

5. Electromagnetic Properties

Since theoretical electromagnetic multipole moments and transition rates depend strongly on the structure of the eigen-vectors, describing the relevant states, the calculation of these properties can serve as a sensitive test for the wave functions extracted in terms of the present model. The wavefunctions employed are those of calculation II, due to its much better data to parameter ratio and its comprehensive nature through the whole mass region.

5.1. Static Nuclear Moments of Ground States

The magnetic dipole and electric quadrupole moments for ground states in the $10 \leq A \leq 14$ mass region have been calculated using free-nucleon g -factors and charges. In Table 3 the results are compared with their experimental analogues, taken from Refs. [3–5, 45, 46].

For all the ground states considered, the calculated values of the $M1$ moments are found to be in excellent agreement with experiment. Confirmation of the uncertain negative phase of the ^{11}C dipole moment is obtained, while the present theory favours a plus sign for the uncertain phase of the ^{12}N dipole moment. As regards the listed $E2$ moments, a major discrepancy in both the phase and magnitude occurs in the case of the $3^+, 0$ ground state of ^{10}B . This failure of the present model is to be expected in view of the difficulty which was encountered to reproduce the binding energy of this level (see Table 1 and Section 4.1). Its $M1$ moment is, however, very accurately accounted for. It is also interesting to note that both the $M1$ and $E2$ moments of the $1^+, 0$ ground state of ^{14}N are well reproduced, in spite of its simple structure in terms of the present model.

Table 3. Static nuclear moments for ground states of nuclei in the $10 \leq A \leq 14$ mass region

A	Nucleus	J^π, T	Magnetic dipole moment (n.m.)		Electric quadrupole moment (b)	
			Experiment	Theory	Experiment	Theory
10	B	$3^+, 0$	+ 1.8007	+ 1.8123	+ 0.08	− 0.0017
11	B	$3/2^-, 1/2$	+ 2.6885	+ 2.8728	+ 0.0372	+ 0.0119
	C	$3/2^-, 1/2$	(−) 1.027	− 1.1041	(+) 0.0308	− 0.0074
12	B	$1^+, 1$	+ 1.003	+ 1.0382		
	N	$1^+, 1$	(\mp) 0.457	+ 0.3475		
13	B	$3/2^-, 3/2$	+ 3.1771	+ 3.2363		
	C	$1/2^-, 1/2$	+ 0.7024	+ 0.7335		
	N	$1/2^-, 1/2$	− 0.3221	− 0.3582		
14	N	$1^+, 0$	+ 0.4036	+ 0.3943	+ 0.0167	+ 0.0126

5.2. Gamma Radiative Widths of Excited States

As a first attempt, the radiative widths have been calculated using free-nucleon gyromagnetic factors for the $M1$ transitions and free charges for the $E2$ transitions which are allowed between natural parity states of $1p$ -shell structure. These results are listed in Tables 4 and 5 and compared with measured values taken from Refs. [3–5].

Although good agreement with experiment is obtained in several cases, the occurrence of many discrepancies, especially in the $E2$ transitions, indicates the need for effective electromagnetic operators. In this way corrections due to the truncation of the shell model basis as well as the schematic nature of the MSDI as two-body interaction can be effected.

Effective values of the electromagnetic operators were therefore obtained from a least-squares fit of the theoretical transition amplitudes to the experimental values of the nuclear moments and transition widths listed in Tables 3–5. In the determination of the relative signs of the amplitudes and the weighing factors for the experimental data, similar criteria as that of Ref. [12] were presently used.

In the magnetic dipole case, fitted values of the effective g -factors were obtained which did not differ significantly from their corresponding free-nucleon values and which did not much improve the calculated $\Gamma(M1)$ values listed in Table 4. For $E2$ transitions and electric quadrupole moments on the other hand, an optimum positive nucleon charge correction have been found in separate fits for different mass nuclei,

Table 4. Magnetic dipole transitions in nuclei with $10 \leq A \leq 14$

Nu- cleus	Initial state		Final state		Radiative width $\Gamma(M1)$ (eV)	
	$J_i^\pi, T_i(N_i)$	E_{xi} (MeV)	$J_f^\pi, T_f(N_f)$	E_{xf} (MeV)	Theory	Experiment
^{10}B	$0^+, 1(1)$	1.74	$1^+, 0(1)$	0.717	8.9×10^{-2}	4.4×10^{-3}
	$1^+, 0(2)$	2.15	$0^+, 1(1)$	1.74	2.2×10^{-3}	(2.5×10^{-4})
	$1^+, 0(3)$	5.18	$0^+, 1(1)$	1.74	0.7×10^{-1}	0.6
^{11}B	$3/2^-, 1/2(2)$	5.02	$3/2^-, 1/2(1)$	0	1.68	1.73 ± 0.14
	$3/2^-, 1/2(3)$	8.57	$3/2^-, 1/2(1)$	0	0.13×10^{-1}	0.72 ± 0.30
	$5/2^-, 1/2(2)$	8.93	$3/2^-, 1/2(1)$	0	5.4×10^{-1}	4.0 ± 0.6
^{13}C	$3/2^-, 1/2(1)$	3.68	$1/2^-, 1/2(1)$	0	0.604	0.358 ± 0.045
	$1/2^-, 1/2(2)$	8.86	$1/2^-, 1/2(1)$	0	0.816	3.36 ± 0.46
	$3/2^-, 1/2(2)$	9.90	$1/2^-, 1/2(1)$	0	$0.367 \times 10^{+1}$	0.324 ± 0.05
	$1/2^-, 1/2(3)$	11.08	$1/2^-, 1/2(1)$	0	$1.33 \times 10^{+1}$	1.02 ± 0.20
^{14}N	$0^+, 1(1)$	2.31	$1^+, 0(1)$	0	1.5×10^{-1}	$(7.7 \pm 1.0) \times 10^{-3}$
	$1^+, 0(2)$	3.95	$1^+, 0(1)$	0	9.6×10^{-3}	$(5.8 \pm 1.2) \times 10^{-4}$
			$0^+, 1(1)$	2.31	0.17	0.14 ± 0.013
	$2^+, 0(1)$	7.02	$1^+, 0(1)$	0	9.1×10^{-2}	$(9.1 \pm 1.3) \times 10^{-2}$

Table 5. Electric quadrupole transitions in nuclei with $10 \leq A \leq 14$

Nu- cleus	Initial state		Final state		Radiative width $\Gamma(E2)$ (eV)		
	$J_i^\pi, T_i(N_i)$	E_{xi} (MeV)	$J_f^\pi, T_f(N_f)$	E_{xf} (MeV)	Theory		Experiment
					Free charge	Effective charge	
^{10}B	$1^+, 0(1)$	0.72	$3^+, 0(1)$	0	8.3×10^{-8}	3.3×10^{-7}	6.6×10^{-7}
	$1^+, 0(2)$	2.15	$3^+, 0(1)$	0	3.0×10^{-6}	1.0×10^{-5}	(1.1×10^{-4})
	$2^+, 0(1)$	3.59	$0^+, 1(1)$	1.74	1.2×10^{-6}	1.2×10^{-6}	$(< 2.1 \times 10^{-4})$
	$3^+, 0(2)$	4.77	$1^+, 0(1)$	0.717	0.058×10^{-2}	0.023×10^{-1}	0.028
^{10}C	$2^+, 1(1)$	3.36	$0^+, 1(1)$	0	3.2×10^{-4}	5.0×10^{-4}	4.2×10^{-3}
^{10}Be	$2^+, 1(1)$	3.37	$0^+, 1(1)$	0	7.7×10^{-5}	1.8×10^{-5}	(4.3×10^{-3})
^{11}B	$3/2^-, 1/2(2)$	5.02	$3/2^-, 1/2(1)$	0	0.0007	0.0010	< 0.0034
	$3/2^-, 1/2(3)$	8.57	$3/2^-, 1/2(1)$	0	0.0003	0.004	0.40 ± 0.10
^{12}C	$2^+, 0(1)$	4.43	$0^+, 0(1)$	0	1.55×10^{-3}	6.2×10^{-3}	$(11.7 \pm 0.5) \times 10^{-3}$
^{13}C	$3/2^-, 1/2(1)$	3.68	$1/2^-, 1/2(1)$	0	0.71×10^{-3}	3.09×10^{-3}	$(3.61 \pm 0.39) \times 10^{-3}$
	$5/2^-, 1/2(1)$	7.55	$1/2^-, 1/2(1)$	0	0.040	0.116	0.115 ± 0.006
	$3/2^-, 1/2(2)$	9.90	$1/2^-, 1/2(1)$	0	9.7×10^{-3}	9.6×10^{-3}	$(6.3 \pm 0.21) \times 10^{-3}$
^{14}N	$1^+, 0(2)$	3.95	$1^+, 0(1)$	0	1.00×10^{-3}	4.34×10^{-3}	$(4.81 \pm 0.33) \times 10^{-3}$
	$2^+, 0(1)$	7.02	$1^+, 0(1)$	0	1.5×10^{-2}	6.3×10^{-2}	$(3.3 \pm 0.9) \times 10^{-2}$
			$0^+, 1(1)$	2.31	3.5×10^{-4}	4.5×10^{-4}	$(6.2 \pm 1.4) \times 10^{-4}$
	$2^+, 1(1)$	9.17	$0^+, 1(1)$	2.31	0.01	0.04	0.11 ± 0.4

which generally varied around $\sim 0.5e$ for both protons and neutrons. Therefore Table 5 also presents the $E2$ strengths, recalculated with $e_p = 1.5e$ and $e_n = 0.5e$. These strengths reproduce the experimental values much better, even in the worst case of disagreement, i.e. the ^{10}B nucleus. These effective charges are similar to those previously used in shell-model calculations for light nuclei (see Refs. [11, 13]).

6. Summary

In the present work an attempt has been made to account for some of the observed properties of natural parity states in the $10 \leq A \leq 14$ nuclei in terms of a pure $1p$ shell model. With regard to the effective two-body interaction between the nucleons outside the ^4He core, it has been found possible to describe all two-particle interactions of the $1p$ shell in terms of only three parameters, using a schematic zero-range surface force, instead of fitting fifteen effective matrix elements as in the calculations of Cohen and Kurath [1]. Two of these three MSDI parameters account for the strength of the two-body interaction, which slightly increases with mass number. The inclusion of an additional third parameter is

essential in order to give a simultaneous description of groups of levels with different isospin. This modification parameter is a direct measure of the strength of a scalar isospin force $B(\tau_i \cdot \tau_j)$ and remains reasonably constant over the mass region considered. The optimum single-particle energy splittings $E(1p_{1/2}) - E(1p_{3/2})$ for the different mass numbers agree well with those of Halbert *et al.* [2]. The level systematics of natural parity states in the mass region considered are generally well reproduced. Unique spin and parity assignments are obtained in some cases where experimental ambiguities still exist; e.g. the 8.57 MeV and 8.11 MeV mirror levels in ^{11}B and ^{11}C respectively ($3/2^-$), and the 10.30 MeV state in $^{12}\text{C}(0^+)$.

Although the truncation of the shell model space in the present investigation does not allow for $2s-1d$ admixing to the pure $1p$ configurations, even near the upper end of the $1p$ shell, a number of measurable quantities are predicted. The experimental binding and excitation energies are well reproduced, especially so in the case of the odd- A nuclei. The magnetic dipole moments of the ground states are predicted in excellent agreement with their corresponding empirical values, and without the need to allow for core-polarization effects and higher shell model orbits. Such a good agreement could, however, not be obtained for $M1$ -transitions between the excited states. This implies that the present truncated model space seems to describe the ground states quite well, but, if higher states are excited, the effect of the $2s-1d$ shell becomes more and more significant. This means that proper use of effective electromagnetic parameters can only be obtained if these parameters are slightly varied with mass number and also with excitation within a certain nucleus. This would of course require a mass of transition data, which is not yet available. The $E2$ radiative widths were found to be in good overall agreement with their measured counterparts when an increment of $\sim 0.5 e$ is added to both the proton and neutron charge.

The authors are very much indebted to Drs. P. W. M. Glaudemans and J. F. A. van Hienen of the Fysisch Laboratorium der Rijksuniversiteit, Utrecht, Netherlands for helpful preliminary discussions as well as for availing some of their shell-model codes. Professor W. Greiner of the Institut für Theoretische Physik der Universität Frankfurt/M., Germany is thanked for his valuable criticism of the results of this investigation.

References

1. Cohen, S., Kurath, D.: Nucl. Phys. **73**, 1 (1965); Nucl. Phys. A **101**, 1 (1967)
2. Halbert, E. C., Kim, Y. E., Kuo, T. T. S.: Phys. Lett. **20**, 657 (1966)
3. Lauritsen, T., Ajzenberg-Selove, F.: Nucl. Phys. **78**, 1 (1966)
4. Ajzenberg-Selove, F., Lauritsen, T.: Nucl. Phys. A **114**, 1 (1968)
5. Ajzenberg-Selove, F.: Nucl. Phys. A **152**, 1 (1970)

6. Glaudemans, P. W. M., Wildenthal, B. H., McGrory, J. B.: Phys. Lett. **21**, 427 (1966)
7. Wildenthal, B. H., McGrory, J. B., Halbert, E. C., Glaudemans, P. W. M.: Phys. Lett. **27 B**, 611 (1968)
8. Glaudemans, P. W. M., Dieperink, A. E. L., Keddy, R. J., Endt, P. M.: Phys. Lett. **28 B**, 645 (1969)
9. Engelbertink, G. A. P., Glaudemans, P. W. M.: Nucl. Phys. A **123**, 225 (1969)
10. Dieperink, A. E. L., Glaudemans, P. W. M.: Phys. Lett. **28 B**, 531 (1969)
11. Maripuu, S., Hokken, G. A.: Nucl. Phys. A **141**, 481 (1970)
12. Glaudemans, P. W. M., Endt, P. M., Dieperink, A. E. L.: Ann. Phys. (N. Y.) **63**, 134 (1971)
13. Wildenthal, B. H., McGrory, J. B., Glaudemans, P. W. M.: Phys. Rev. Letters **26**, 96 (1971)
14. De Voigt, M. J. A.: Thesis for the degree Dr. Wisk. Nat., Rijksuniversiteit of Utrecht (1972)
15. MacFarlane, M. H., French, J. B.: Rev. Mod. Phys. **32**, 567 (1960)
16. De-Shalit, A., Talmi, I.: Nuclear shell theory. New York: Academic Press 1963
17. Glaudemans, P. W. M., Wiechers, G., Brussaard, P. J.: Nucl. Phys. **56**, 529, 548 (1964)
18. Plastino, A., Arvieu, R., Moszkowski, S. A.: Phys. Rev. **145**, 837 (1966)
19. Glaudemans, P. W. M., Brussaard, P. J., Wildenthal, B. H.: Nucl. Phys. A **102**, 593 (1967)
20. Fisher, T. R., Hanna, S. S., Healey, D. C., Paul, P.: Phys. Rev. **176**, 1130 (1968)
21. Nellis, D. O., Tucker, W. E., Morgan, T. L.: Phys. Rev. C **1**, 843 (1970)
22. Ling, S. C., Blatt, S. L.: Nucl. Phys. A **174**, 375 (1971)
23. Young, F. C., Lindgren, R. A., Reichart, W.: Nucl. Phys. A **176**, 289 (1971)
24. Cospers, S. W., McGrath, R. L., Cerny, J., Maples, C. C., Goth, G. W., Fleming, D. G.: Phys. Rev. **176**, 1113 (1968)
25. Fortune, H. T., Comfort, J. R., Maher, J. V., Zeidman, B.: Phys. Rev. C **2**, 425 (1970)
26. Comfort, J. R., Fortune, H. T., Maher, J. V., Zeidman, B.: Phys. Rev. C **3**, 1086 (1971)
27. Lane, R. O., Hausladen, S. L., Monahan, J. E., Elwyn, A. J., Mooring, F. P., Langsdorf, A., Jr.: Phys. Rev. C **4**, 380 (1971)
28. Watson, B. A., Chang, C. C., Hasinoff, M.: Nucl. Phys. A **173**, 634 (1971)
29. Ball, G. C., Cerny, J.: Phys. Rev. **177**, 1466 (1969)
30. Bohne, W., Hagen, M., Homeyer, H., Maier, K. H., Lettau, H., Morgenstern, H., Scheer, J.: Phys. Rev. C **2**, 2072 (1970)
31. Lane, R. O., Nelson, C. E., Adams, J. L., Monahan, J. E., Elwyn, A. J., Mooring, F. P., Langsdorf, A., Jr.: Phys. Rev. C **2**, 2097 (1970)
32. Monahan, J. E., Fortune, H. T., Vincent, C. M., Segel, R. E.: Phys. Rev. C **3**, 2192 (1971)
33. Reynolds, G. M., Rundquist, D. E., Pochar, R. M.: Phys. Rev. C **3**, 442 (1971)
34. Hsu, T. H., Honsaker, J. L., McDonald, W. J., Neilson, G. C.: Nucl. Phys. A **174**, 365 (1971)
35. Jäger, H. U., Kissener, H. R., Eramzhian, R. A.: Nucl. Phys. A **171**, 1, 584 (1971)
36. Mikoshiba, O., Terasana, T., Tanifuji, M.: Nucl. Phys. A **168**, 417 (1971)
37. Duray, J. R., Browne, C. P.: Phys. Rev. C **3**, 1867 (1971)
38. Fortune, H. T., Middleton, R., Garrett, J. D., Holbrow, C. H.: Phys. Rev. C **3**, 1441 (1971)
39. Fleming, D. G., Hardy, J. C., Cerny, J.: Nucl. Phys. A **162**, 225 (1971)
40. Kaschl, G., Mairle, G., Mackh, H., Hartwig, D., Schwinn, U.: Nucl. Phys. A **178**, 275 (1971)

41. Cookson, J. A.: Nucl. Phys. A **180**, 89 (1972)
42. Warburton, E. K., Chase, L. F., Jr.: Nucl. Phys. **34**, 517 (1962)
43. Kurath, D.: Phys. Rev. **101**, 216 (1956)
44. True, W. W.: Phys. Rev. **130**, 1530 (1963)
45. Fuller, G. H., Cohen, V. W.: Nuclear moments, appendix I to nuclear data sheets. New York: Academic Press 1965
46. Lindgren, I.: In α -, β - and γ -ray spectroscopy, ed. K. Siegbahn, vol. 2, p. 1621. Amsterdam: North-Holland 1965

Dr. R. Saayman
Dr. P. R. de Kock
Prof. J. H. van der Merwe
Merensky Institute for Physics
University of Stellenbosch
Stellenbosch
South Africa